

# USING FIELD BUOY DATA TO STUDY ASYMMETRICAL WAVE-WAVE INTERACTIONS IN A HORSE-SHOE PATTERN

Ray-Qing Lin<sup>1</sup> and Lihwa Lin<sup>2</sup>

<sup>1</sup> Seakeeping Department, David Taylor Model Basin  
NSWC Carderock Division

<sup>2</sup> Coastal and Hydraulics Laboratory  
U.S. Army Engineer Research and Development Center

## 1. INTRODUCTION

“Horseshoe” patterns are often observed on the ocean surface. Kalmykov (1999) suggests that these “horseshoe” patterns are generated by coupled 4-wave and 5-wave interactions. According to Kalmykov (1999), the indirect cascades result from 4-wave interactions and direct cascades result from 5-wave interactions. However, 5-wave interactions are generally two-orders of magnitude smaller than 4-wave interactions, except when wave steepness exceeds 0.28, (McLean, 1982; Su, 1982a and 1982b; Lin and Perrie, 1997 and 1999). If Kalmykov is correct, the “horseshoe” pattern can only occur when the wave steepness is large, and the “horseshoe” pattern will appear regardless of whether an initial spectrum is symmetrical or not.

However, in the International Competition in the Base Enhancement Wave Prediction Conference in Mississippi in 1998, the nonlinear energy transfer rates of weak nonlinear 4-wave interaction models by Hasselmann and Hasselmann, (1981); Resio and Tracy, (1998); Lin and Perrie, (1997 and 1999), all produced “horseshoe” patterns for an initial wave spectrum that is directionally split. To understand the mechanism responsible for the “horseshoe” pattern, we investigate sea wave measurements. Our choice is the directional buoy data collected by the National Data Buoy Center (NDBC), the quality of which, in general, is good for showing wave energy transfer patterns. The NDBC buoys measure directional waves by recording roll and pitch on the surface. The buoy data can be analyzed to describe directional wave energy distributions with second order accuracy. In this study, the analysis of directional buoy data is based on the Maximum Entropy method (Kim, *et al.*, 1993; Lin, *et al.*, 1996). The primary use of the buoy data is to derive the energy transfer features associated with the data and to examine the asymmetric nature of wave-wave interactions in the “horseshoe” pattern.

## 2. BUOY OBSERVATIONS

The NDBC buoy data are normally collected on an hourly basis. To determine the nonlinear transfer rate from buoy data, it is important to select the cases with rather weak and constant winds to eliminate the varying wind input effect.

Following the above principle, wave data observed from NDBC Buoys 51026, 41009, and 42003 were randomly chosen to study the nonlinearity of energy transfer. Buoy 50126 is located approximately 20km north of Molokai, Hawaii, at a normal depth of 2300 m. Buoy 41009 is located approximately 25 km east of Cape Canaveral, FL, on the continental shelf of the Atlantic Ocean at a normal depth of 2000m. Buoy 42003 is located at the geometric center of the eastern Gulf of Mexico in a normal depth of 3100 m. These three buoys were located in three different ocean regions, i.e., one in the Pacific Ocean, the second in the Atlantic Ocean, and the third in the Gulf of Mexico. These buoys were selected to show that the major wave energy transfer mechanism should be the same regardless of location. The three buoys were also chosen because their locations favor weak and constant wind conditions necessary for the investigation of energy transfer pattern.

Using these buoy data, the energy transfer rate can be determined from the difference between two spectra measured in the one-hour interval. This practice allowed many cases to be calculated. For wave-wave interactions, there are numerous cases to demonstrate the energy transfer pattern. Since they are similar in nature, we have simply selected six cases for illustration. These are shown in Figures 1 to 6, which are typical of the energy transfer rates from nonlinear wave-wave interactions.

Figures 1a, 2a, 3a, 4a, 5a, and 6a show the associated initial spectra from Buoy 51026, 41009, and 42003, respectively. Figures 1b to 6b show the examples of energy transfer rates computed from the directional spectra of the same buoys. These examples typify waves generated under the moderate wind condition with a small shift of wind direction. This wind condition is ideal to reveal the pattern of energy transfer rates associated with asymmetric wave-wave interactions.

Figure 1a shows the initial directional split spectrum ( $\text{m}^2/\text{Hz}/\text{rad}$ ) at 12:00 GMT on September 21, 1994 by Buoy 51026 at water depth 2300m. Significant wave height is approximately equal to 1.9 m, peak energy density is  $1 \text{ m}^2/\text{Hz}/\text{rad}$ , and peak frequency is 0.12 Hz. The dispersion relationship for the finite water depth is  $\omega_p^2 = gk_p \tanh k_p h$ , where  $\omega_p$ ,  $k_p$  and  $h$  are the peak frequency, the absolute value of peak wave number, and water depth, respectively, and  $g$  is the gravitational acceleration, equal to  $9.8 \text{ m/s}^2$ . The corresponding wave steepness of the peak wave is  $a_p k_p \tanh kh = 0.0058$ , which is five-times less than the critical value,  $a_p k_p \tanh kh = 0.28$  required for the energy density transfer rate of 5-wave interactions (class II instability) to be equivalent to the 4-wave interactions (class I instability) (Mclean, 1982; Su, 1982a). Therefore, it is impossible for the 5-wave interactions to generate two visible satellite patterns from the initial spectrum in Figure 1a. Only 4-wave interactions with a directionally split initial spectrum can result the satellites.

The nonlinear transfer pattern is examined next for the same buoy data. Figure 1b shows the energy transfer rates between 12:00 and 13:00 GMT. The horizontal coordinate is frequency (Hz) and vertical coordinate is direction (deg). The rate of change of the wave spectral density is shown by contour lines ( $\text{m}^2/\text{Hz}/\text{rad}/\text{hour}$ ). The solid line, indicating positive contours, corresponds to the energy gain and the dashed line, indicating negative contours, corresponds to the energy loss. From 12:00 to 13:00 GMT, the wind direction changes from  $269^\circ$  to  $271^\circ$  and wind magnitude decreases slightly from 11 m/s to 10 m/s. The maximum positive energy transform appears at 0.125 Hz and  $263^\circ$ . The maximum negative energy transform appears at 0.15 Hz and  $271^\circ$ . The indirect cascades (energy transfer from high frequency to low frequency) dominate in the energy transfer during 12:00 to 13:00 GMT. The high frequency negative transform is exactly in the down wind direction, whereas the positive energy transform is on the left side of the down wind direction. There is an oblique positive energy transform located at 0.16 Hz and  $235^\circ$  on the same side of the positive energy transform.

Another example of the initial directionally split spectrum from Buoy 51026, recorded at 21:00 GMT on September 19, 1994 is shown in Figure 2a. The significant wave height is 1.9 m, peak energy density is  $0.2 \text{ m}^2/\text{Hz}/\text{rad}$ , and peak frequency is 0.11 Hz. The wave steepness,  $a_p k_p \tanh kh = 0.00975$ , is almost two-orders of magnitude smaller than the critical value,  $ak \tanh kh = 0.28$ . Therefore, Kalmykov's theory predicts no satellites, whereas the 4-wave interactions theory predicts satellites. Figure 2b shows the energy transfer rates related to Figure 2a, from 21:00 to 22:00 GMT. Within the one-hour interval, the wind direction changed from  $277^\circ$  to  $276^\circ$  and the wind speed increased from 11 to 12 m/s. The positive energy transform is at 0.21 Hz and  $260^\circ$  and the negative energy transform is at 0.25 Hz and  $280^\circ$ . This indicates that the indirect cascades dominate the energy transform. A small oblique positive energy transform satellite is visible at 0.245 Hz and  $240^\circ$  on the same side of the maximum positive energy transform.

The third example is shown in Figure 3a. The initial directionally split spectrum was recorded at 6:00 GMT on October 2, 1993 by Buoy 41009. The significant wave height is 1.6 m, peak wave energy density is  $0.8 \text{ m}^2/\text{Hz}/\text{rad}$ , and peak frequency is 0.13 Hz. The initial spectrum's wave steepness is  $a_p k_p \tanh kh = 0.055$ , which is 5-times smaller than the critical value,  $ak \tanh kh = 0.28$ , (Mclean, 1982; Su, 1982a). Again, Kalmykov's theory predicts no satellites, but 4-wave interactions theory predicts satellites. The corresponding energy transfer rates, associated with the initial spectrum in Figure 3a, are shown in Figure 3b for the time period from 6:00 to 7:00 GMT. The wind direction changed from  $256^\circ$  at 6:00 GMT to  $262^\circ$  at 7:00 GMT while the wind magnitude remained the same at 8 m/s. A strong positive energy transform appears at 0.13 Hz and  $262^\circ$ . The corresponding negative energy transforms appear in the higher frequency range between 0.14 and 0.17 Hz at  $240^\circ$ . This indicates that the indirect cascades dominate the energy transform. There are two oblique positive satellites shown on the same side of the positive energy transform. One is located at 0.17 Hz,  $290^\circ$  and the other is located at 0.2 Hz,  $270^\circ$ .

The fourth example is also from Buoy 41009. The initial directional spectrum at 0:00 GMT on December 1, 1993 is shown in Figure 4a. The significant wave height is 2.0 m, peak wave energy density is  $0.2 \text{ m}^2/\text{Hz}/\text{rad}$ , and peak frequency is 0.09 Hz. The peak wave steepness,  $a_p k_p \tanh kh = 0.0326$ , is about one-order smaller than the critical

value, so Kalmykov's theory predicts no satellites. However, the 4-wave interactions theory predicted the satellites. The nonlinear transfer rate pattern from 0:00 to 1:00 GMT is shown in Figure 4b. During this one-hour interval, the wind direction has changed from  $224^\circ$  to  $227^\circ$  while wind magnitude remained the same at 11 m/s. The maximum positive energy transform appears at 0.15 Hz and  $210^\circ$  on the left side of the down wind direction. There are two corresponding maximum negative energy transforms. They are located at 0.2 Hz,  $240^\circ$  and at 0.24 Hz,  $230^\circ$  on the right side of the down wind direction. A small positive energy transform satellite appears at 0.19 Hz and  $180^\circ$ , on the same side of the maximum positive energy transform.

The fifth example is shown in Figures 5, where initial directionally split spectrum at 12:00 GMT on July 22, 1992 was recorded by Buoy 42003. The significant wave height is 0.6 m, spectral peak energy is  $0.03 \text{ m}^2/\text{Hz}/\text{rad}$ , and peak frequency is 0.17 Hz. The peak wave steepness,  $a_p k_p \tanh kh = 0.0035$  is 2-orders of magnitude smaller than the critical value. Again, Kalmykov's theory predicts no satellites, whereas, the 4-wave interaction theory predicts satellites. The energy transfer rates from 12:00 to 13:00 GMT are shown in Figure 5b. The maximum positive energy transform appears at 0.18 Hz and  $275^\circ$ . The corresponding maximum negative energy transform appears at 0.22 Hz and  $300^\circ$ . Wind direction changed from  $308^\circ$  at 12:00 GMT to  $297^\circ$  at 13:00 GMT while wind magnitude remains the same at 6 m/s. An oblique positive satellite appears on the same side of the positive energy transform at 0.22 Hz and  $250^\circ$ . The maximum positive energy transform extends towards the oblique positive satellite and form a secondary positive energy transform at 0.2 Hz as a result of relatively large change in the wind direction. The indirect cascades dominate the case.

Figure 6a shows the last example of the directionally split spectrum at 3:00 GMT on January 2, 1993 by Buoy 42003. The significant wave height is 1.5 m, spectral peak energy is  $0.3 \text{ m}^2/\text{Hz}/\text{rad}$ , and peak frequency is 0.19 Hz. The peak wave steepness is  $a_p k_p \tanh kh = 0.031$  and is about one-order magnitude smaller than the critical value. The energy transfer rates between 3:00 to 4:00 GMT are shown in Fig. 6b during which wind direction changed from  $226^\circ$  to  $225^\circ$  and wind speed increased from 10 m/s to 11 m/s. The maximum positive energy transform appears at 0.155 Hz and  $190^\circ$ . The maximum negative energy transforms appears at 0.19 Hz and  $220^\circ$ . A relatively large positive satellite is seen at 0.21 Hz and  $210^\circ$  on the same side of the maximum positive energy transform.

Figures 1a to 6a show that the initial spectra are all directionally split with the wave steepness,  $a_p k_p \tanh k_p h \ll 0.28$ . The energy transfer patterns in Figures 1b to 6b have shown some similar features: the central harmonic patterns are indirect cascade, and the oblique satellites are direct cascades. The central harmonics always dominate and associate with oblique satellites. The buoy data show clearly that the "horseshoe" pattern occurs even when the wave steepness is very small. The buoy data also show that the oblique positive satellite is always associated with the central harmonics. These asymmetrical nonlinear energy transfers in wave number space can cause the symmetrical "horseshoe" pattern in the water surface space as often observed on the ocean surface (Lin and Kuang, 2001). These evidences indicate that the "horseshoe" pattern is mainly caused by 4-wave interactions when the initial spectrum is directionally split. The central harmonic pattern is due to the indirect cascades of 4-wave interactions and the oblique satellites are due to the direct cascades of 4-wave interactions when the initial spectrum is directionally split. The directionally split wave spectrum exists because the wind direction changes. Therefore, the "horseshoe" pattern is frequently observed in the field.

### 3. PHYSICAL MODELS

#### 3.1 5-Wave Interactions

Kalmykov (1999) suggested Class I instabilities, such as four-, six-, ... wave-wave interactions are indirect cascades, which is the energy transfer from high frequency to low frequency. But Class II instabilities, such as five-, seven-, ... wave interactions are direct cascades, which is the energy transfer from low frequency to high frequency. According to Kalmykov (1999), these direct cascades of 5-wave interactions are the mechanism of the positive oblique satellites of the "horseshoe" pattern. His typical pattern is showed in the Figure 7. He concluded that the "horseshoe" patterns occur due to coupled 4- and 5-wave interactions. The mechanism of 4-wave interactions is of positive central harmonics. The 5-wave interactions are usually one-, or two-orders smaller than 4-wave interactions, as the buoy data showed in the last section, because the wave steepness is usually much smaller than the critical value, 0.28. Therefore, according to Kalmykov's theory, satellites shown in the Figure 7 cannot exist. However, Figures 1b to 6b actually show that "horseshoe" patterns with the central harmonics and oblique satellites do exist. The magnitude of the initial spectrum wave steepness is generally one- to two- orders smaller than the

critical value for 5-wave interactions to be equivalent to the 4-wave interactions. Therefore, the mechanism proposed by Kalmykov is incorrect.

### 3.2 Weak Nonlinear 4-wave Interactions

When an initial wave spectrum is directionally split, all exact solution models, such as those of Hasselmann and Hasselmann, (1981); Resio and Tracy, (1998); Lin and Perrie, (1997 and 1999), predicted a “horseshoe” pattern in the International Competition at the Base Enhancement Wave Prediction Conference in Mississippi in 1998. Their indirect, and direct cascades of 4-directionally split wave interactions induce explicitly the central harmonics and oblique positive satellites of the “horseshoe” pattern, even though they had not discussed the “horseshoe” mechanism. Figure 8 shows the typical pattern from their models. The major difference between Figures 1b to 6b and Figure 8 is that the direct energy transfer in Figure 8 is somewhat more symmetric than that in Figures 1b to 6b.

The agreements between Figures 1b to 6b and Figure 8 are

- (1) Indirect cascades in the central harmonics dominate.
- (2) The oblique satellite appears regardless of whether the wave steepness is large or small.
- (3) The initial spectra are directionally split.

Therefore, the mechanism should be accepted, except for the symmetry of oblique satellites. The symmetry appearing in Figure 8 may be due to the fact that all of the exact solution models assume symmetry.

## 4. CONCLUSIONS:

The buoy observation shows that the “horseshoe” pattern often occurs even if the wave steepness is much smaller than the critical value, 0.28. The main condition for this phenomenon to occur is the initial spectrum must be directionally split. The major mechanism of this phenomenon is deemed to be 4-wave interactions of directionally split spectra, which agrees well with the results of exact-solution models such as Hasselmann and Hasselmann, (1981); Resio and Tracy, (1998); Lin and Perrie, (1997 and 1999). The gradual change in wind direction can be the main cause of the spectrum being directionally split.

## 5. ACKNOWLEDGEMENT

This work is supported by the grant from the Office of Naval Research under Independent Laboratory Research program at the David Taylor Model Basin, Carderock Division. We also thank the Head of the Seakeeping Department at David Taylor Model Basin, Terry Applebee, who gave many useful comments and suggestions.

## 6. REFERENCES

- Hasselmann, S., K. Hasselmann, 1981: A symmetrical method of computing the nonlinear transfer in a gravity-wave spectrum. *Hamb. Geophys. Einzelschriften Reihe A Wiss. Abhand.*, **52**, 138pp.
- Jensen R. E., D. Resio, R.-Q. Lin, G., Vledder, T. Herbers, B. Tracy, 1998: A report of snl source function computational workshop in Vicksburg, Mississippi, USA.
- Kalmykov, V. A., 1999: Comments on a new coastal; wave model, Part V. Five-wave Interactions. *Journal of Physical Ocean.*, **29**, 2110-2112.
- Kim, T, L. Lin, and H. Wang, 1993: Comparisons of directional wave analysis methods. Waves'93 Ocean wave measurement and analysis, Proceedings of the 2<sup>nd</sup> International Symposium. New Orleans, Louisiana. 554-568.
- Lin, L., S. Schofield, and H. Wang, 1996: Comparison of directional wave data quality from two different monitoring Systems. Proceedings of the 25<sup>th</sup> International Conference of Coastal Engineerin, Orlando, Florida, 643-656.

Lin, R.-Q. and W. Perrie, 1997: A new coastal wave model, Part III. Nonlinear wave-wave interactions. *Journal of Physical Oceans*, **27**, 1813-1826.

Lin, R.-Q. and W. Perrie, 1999: Wave-wave interaction in finite water depth water. *J. of Geophys. Res.*, **104**, No. C5, 11193-11213.

McLean, J. W., 1982: Instabilities of finite-amplitude gravity wave on water of finite depth. *J. Fluid Mech.*, **114**, 331-341.

Resio, D. and B. Tracy, 1998: International nonlinear wave-wave interactions in finite water competition, Vicksburg, Mississippi, held by ONR.

Su, M.-Y., 1982a: Three-dimensional Deep-water Waves, Part I. Experimental measurement of skew and symmetric wave patterns. *J. of Fluid Mech.*, **124**, 73-108.

Su, M.-Y., 1982b: Evolution of groups of gravity waves with moderate to high steepness. *Phys. Fluids*, **25**, 2167-2174.

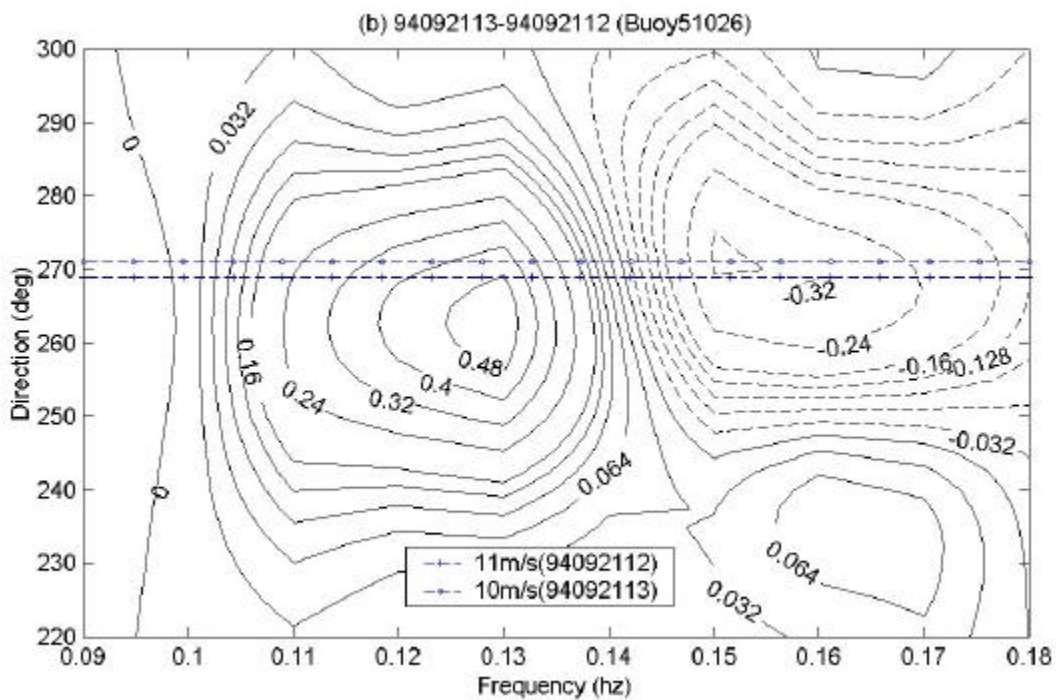
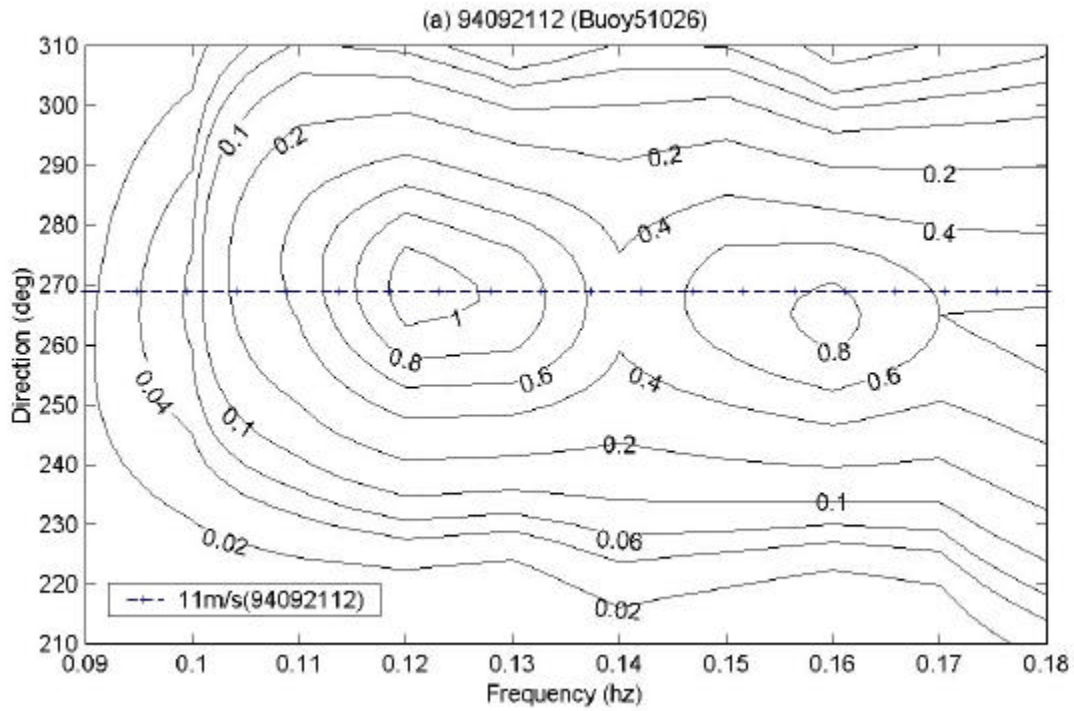


Figure 1. From Buoy 51026 data – (a) initial directional spectrum at 12:00 GMT in September 21, 1994, (b) wave energy transfer rates during 12:00 to 13:00 GMT in September 21, 1994.

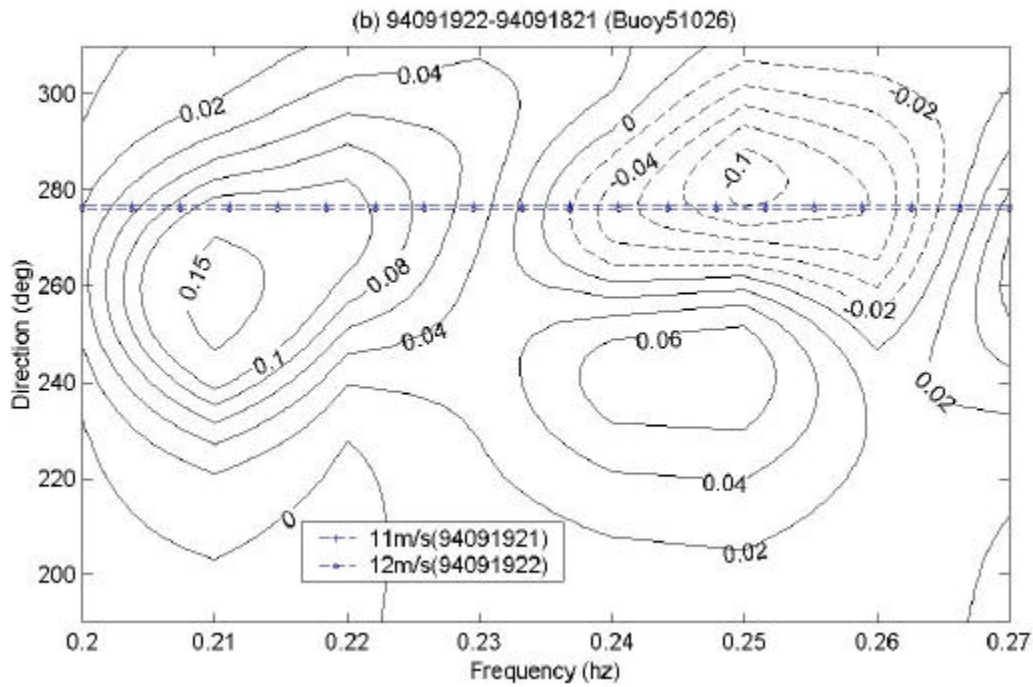
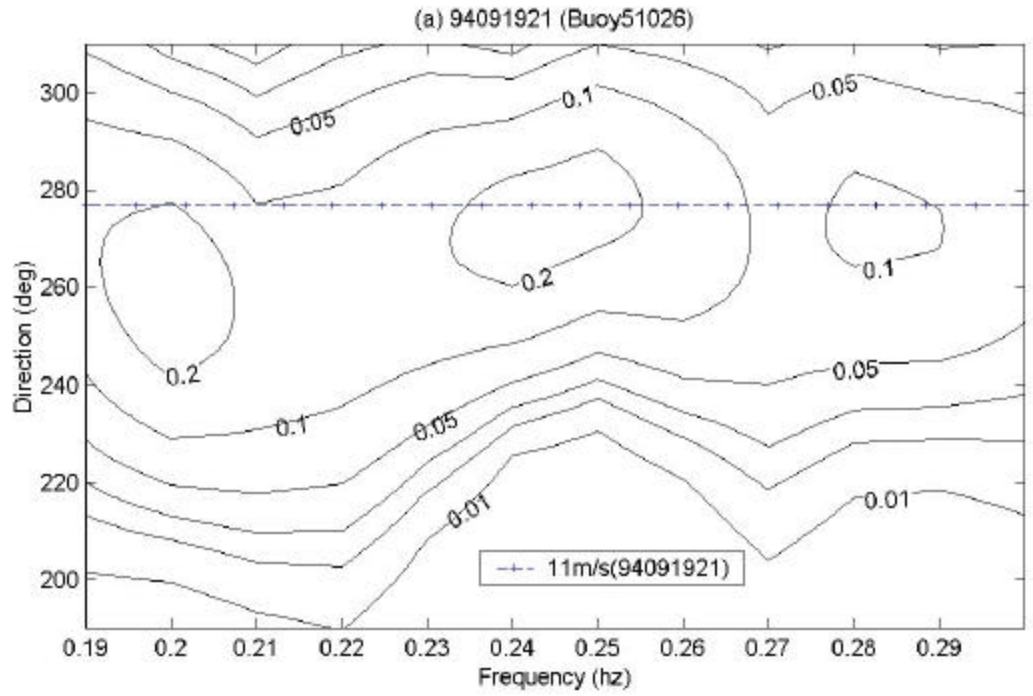


Figure 2. From Buoy 51026 data – (a) initial directional spectrum at 21:00 GMT in September 19, 1994, (b) wave energy transfer rates during 21:00 to 22:00 GMT in September 19, 1994.

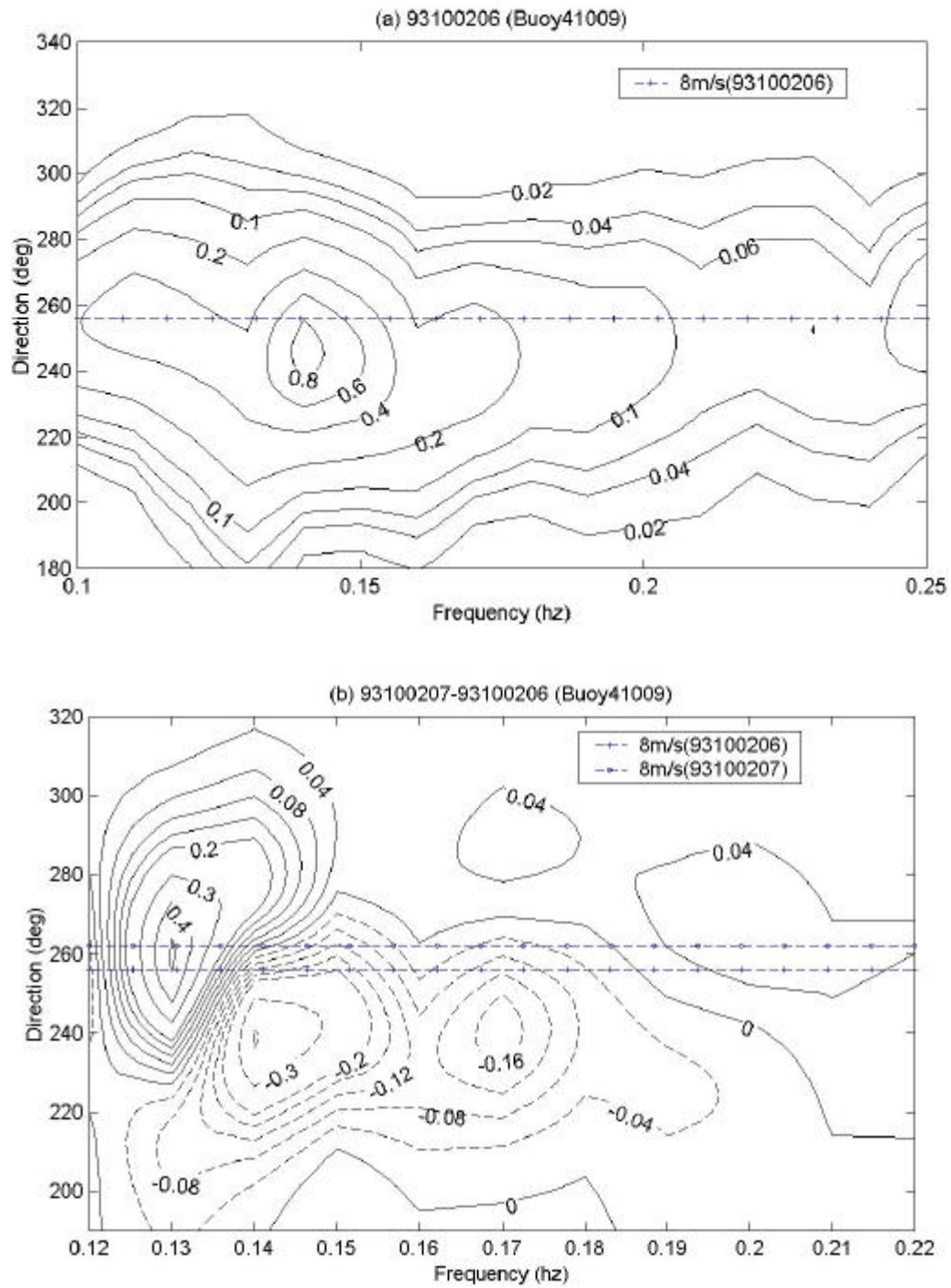


Figure 3. From Buoy 41009 data – (a) initial directional spectrum at 6:00 GMT in October 2, 1993; (b) wave energy transfer rates during 6:00 to 7:00 GMT in October 2, 1993.

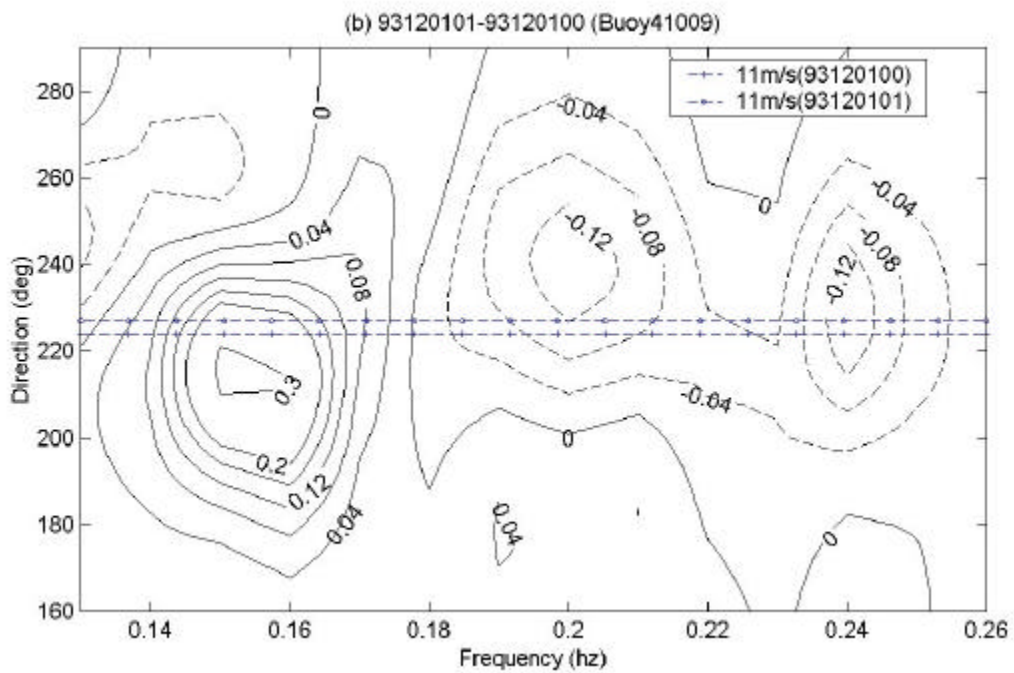
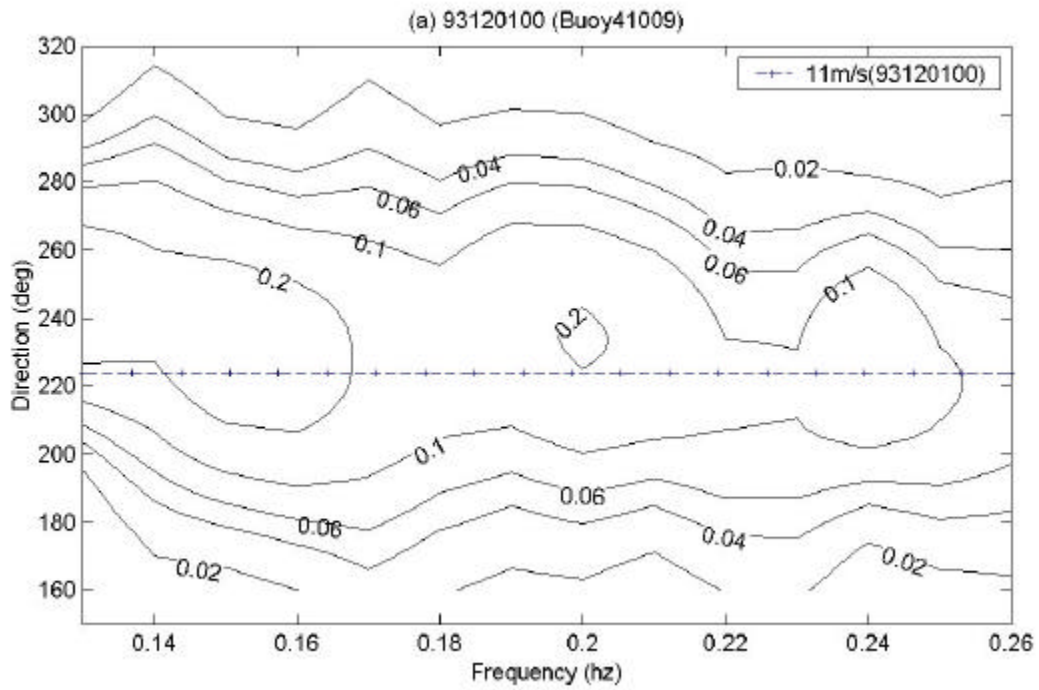


Figure 4. From Buoy 41009 data –(a) initial directional spectrum at 0:00 GMT in December 1, 1993 (b) wave energy transfer rates during 0:00 to 1:00 GMT in December 1, 1993.

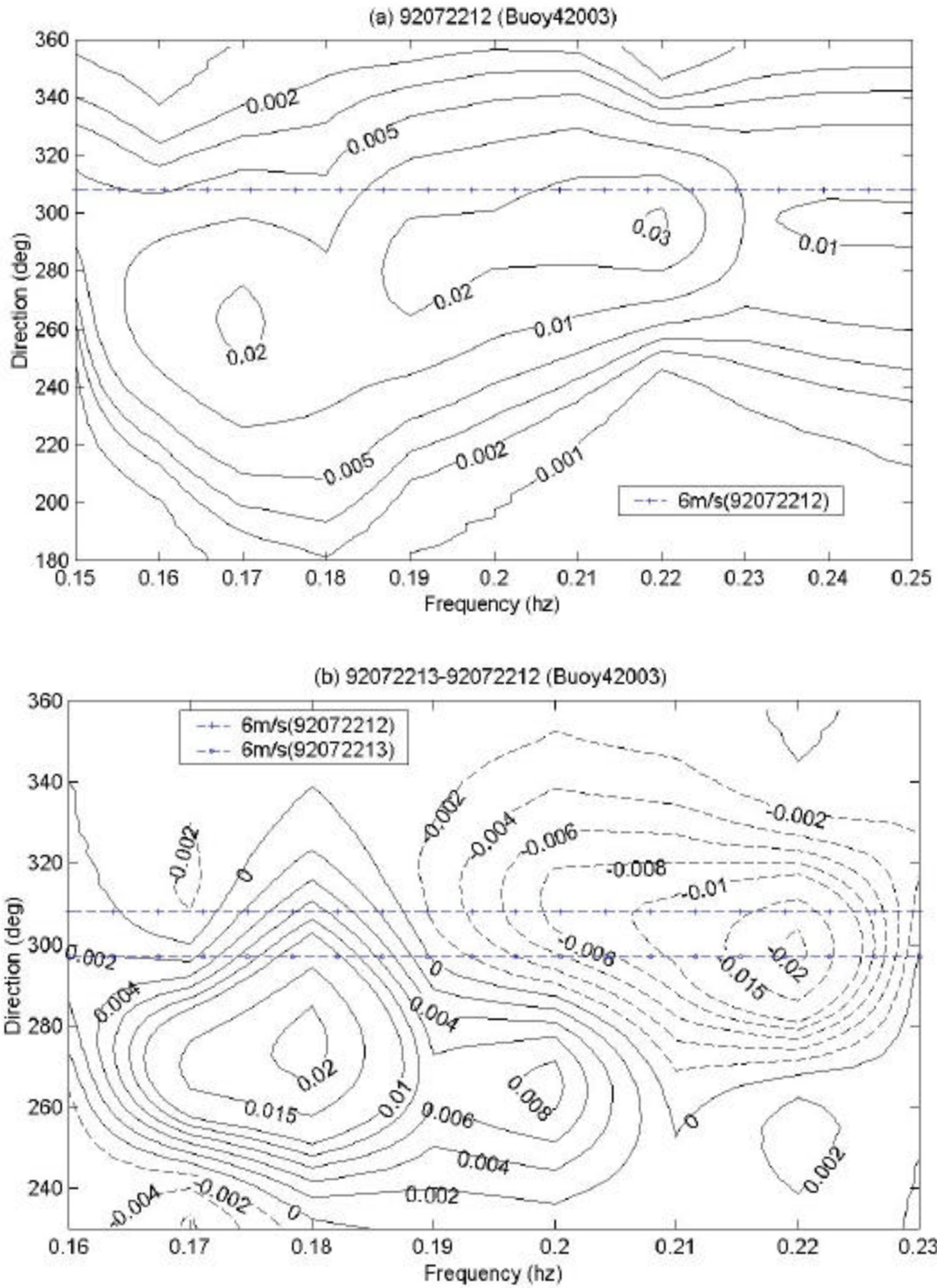


Figure 5. From Buoy 42003 data – (a) initial directional spectrum at 12:00 GMT in July 22, 1992; (b) wave energy transfer rates during 12:00 to 13:00 GMT in July 22, 1992.

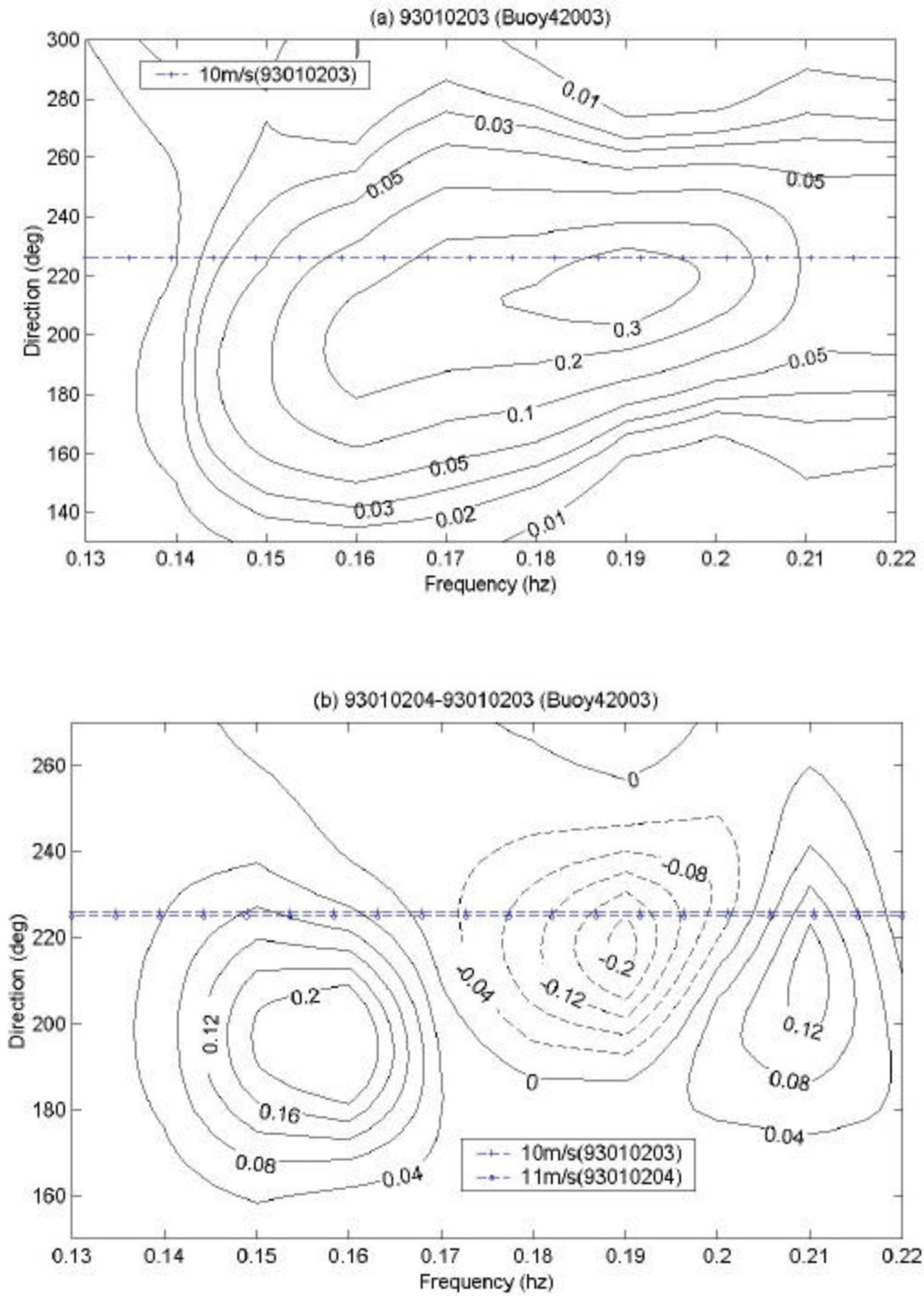


Figure 6. From Buoy 42003 data –(a) initial directional spectrum at 3:00 GMT in January 2, 1993; (b) wave energy transfer rate during 3:00 to 4:00 GMT in January 2, 1993.

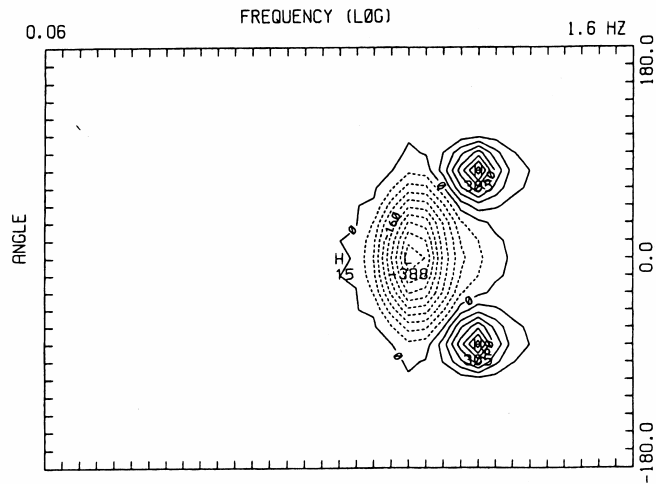


Figure 7. Kalmykov's typical pattern of 5-wave interactions.

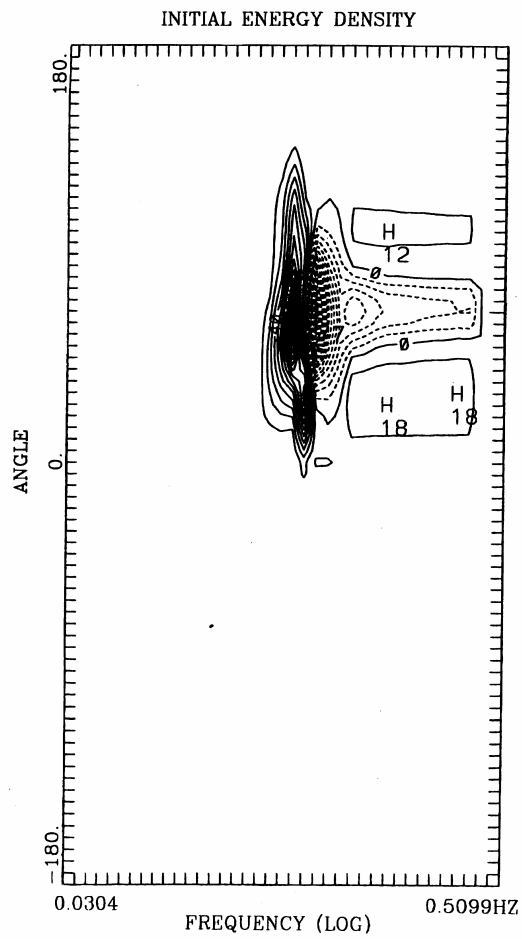


Figure 8. A typical pattern of 4-wave interactions for directional split initial spectrum by Lin and Perrie's reduced Integration Approximation (1999).